Large nonvolatile control of interfacial magnetic anisotropy in CoPt by a ferroelectric ZnO-based tunneling barrier

Muftah Al-Mahdawi,[1,2,3,*] Mohamed Belmoubarik,[3] Masao Obata,[4,†] Daiki Yoshikawa,[4] Hideyuki Sato,[3] Tomohiro Nozaki,[3] Tatsuki Oda,[4,5] and Masashi Sahashi[3,6]

[1]*Center for Science and Innovation in Spintronics (Core Research Cluster), Tohoku University, Sendai 980-8577, Japan*
[2]*Center for Spintronics Research Network, Tohoku University, Sendai 980-8577, Japan*
[3]*Department of Electronic Engineering, Tohoku University, Sendai 980-8579, Japan*
[4]*Graduate School of Natural Science and Technology, Kanazawa University, Kanazawa 920-1192, Japan*
[5]*Institute of Science and Engineering, Kanazawa University, Kanazawa 920-1192, Japan*
[6]*ImPACT Program, Japan Science and Technology Agency, Chiyoda, Tokyo 102-0076, Japan*

(Received 4 October 2018; revised manuscript received 29 June 2019; published 19 August 2019)

The electric control of magnetic anisotropy has important applications for nonvolatile memory and information processing. By first-principles calculations, we show a large nonvolatile control of magnetic anisotropy in the ferromagnetic/ferroelectric CoPt/ZnO interface. Using the switched electric polarization of ZnO, the density-of-states and magnetic anisotropy at the CoPt surface show a large change. Due to a strong Co/Pt orbitals hybridization and a large spin-orbit coupling, a large control of magnetic anisotropy was found. We experimentally measured the change of effective anisotropy by tunneling resistance measurements in CoPt/Mg-doped ZnO/Co junctions. Additionally, we corroborate the origin of the control of magnetic anisotropy by observations on tunneling anisotropic magnetoresistance.

DOI: 10.1103/PhysRevB.100.054423

I. INTRODUCTION

The recent strong interest in the control of magnetism by electric means has been driven by the aspects of fundamental physical understanding of magnetism and more importantly towards applications in nonvolatile information processing in magnetic memories [1,2]. The electric field effect on the interfacial electronic states has been reported to control magnetic Curie temperature T_C [3,4], coercivity H_c [5–7], magnetic moment [8], spin polarization [9], and magnetic anisotropy energy MAE [10,11], both in magnetic semiconductors and transition metals. By using the voltage control of MAE (VCMA), fast writing by nanosecond electric pulses in magnetic tunnel junctions (MTJs) has been widely demonstrated in MTJs based on rock-salt-type MgO barrier [12–14], The main electronic origin of interfacial MAE, and hence VCMA, in an Fe-alloy/MgO system is the orbital hybridization between Fe $3d$ and O $2p$ at the interface in the presence of spin-orbit coupling (SOC) [15]. However, the precise control of Fe surface oxidation is crucial [15] for large MAE and VCMA magnitudes, which are required for nonvolatile memory applications [16–18].

An alternative is the heterostructure of a ferromagnet/ferroelectric (FM/FE) combination [19–23], where a relatively large modulation of MAE is achieved by the control of FE polarization (P). This was shown to be mainly due to the P-dependent hybridization between the orbitals of the FM and FE elements. In this work, we propose and clarify a different mechanism for an FM/FE/FM tunnel junction system to achieve a large nonvolatile control of MAE. We investigated FE-MTJs made from fcc-CoPt FM and wurtzite-ZnO FE, using first-principles calculations and magnetotransport measurements.

An important aspect of $3d$-$5d$ magnetic alloys is that MAE originates from the large SOC of the $5d$ element which is magnetized by the strong exchange field of $3d$ moments [24–26]. In CoPt [24,27], a large MAE along the (1 1 1) crystal axis is retained even under disorder [28]. At the composition near $CoPt_3$, the MAE can be controlled by the growth temperature [24,28–30]. Furthermore, Pt-rich CoPt is suitable for the c-axis growth of wurtzite-type ZnO due to the small lattice mismatch and low interdiffusion with the ZnO layer [31–33]. The wurtzite-type ZnO is a polar semiconductor, where the electric dipoles of buckled Zn-O ions are aligned along the (0 0 0 1) direction. The P reversal changes the chemical potential at the interface that should have a prominent effect on MAE due to the large $5d$ SOC [34]. Therefore, the system of CoPt (1 1 1)/ZnO (0 0 0 1) has a strong potential for a large modulation of MAE.

Based on symmetry point group consideration, ZnO should not possess ferroelectricity. However, further theoretical considerations support the presence of ferroelectricity in wurtzite-like structures [35], mediated by a rotation of the buckled-ions plane through a nonpolar intermediate state [36,37]. Experimentally, ZnO films exhibited ferroelectricity, either vacancy-driven [38] or by doping with various elements [39–44]. Most notably for tunnel barrier fabrication, Mg doping lowers the free carriers concentration and enhances insulating property

*mahdawi@mlab.apph.tohoku.ac.jp
†obata@cphys.s.kanazawa-u.ac.jp

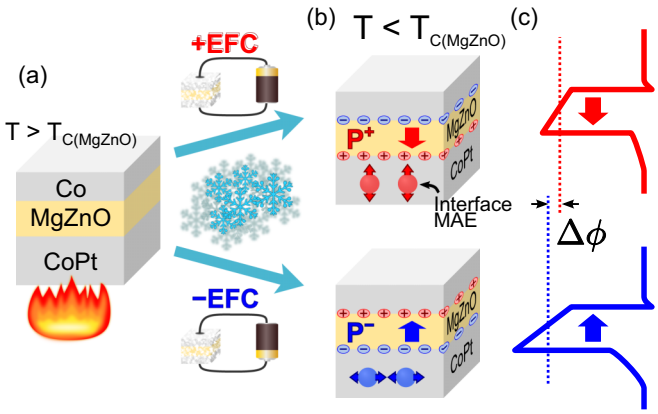

FIG. 1. (a) A schematic of the MgZnO magnetic tunnel junction (MTJ) and the electric-field cooling (EFC) procedure. (b) The reversal of MgZnO electric polarization (P) after EFC changes the surface charge at the metal interfaces of the MTJ. The charge difference is negative (positive) at the CoPt surface after +EFC (−EFC). Correspondingly, the surface MAE of CoPt is perpendicular (in-plane) for P^+ (P^-) states. (c) Schematics of the MTJ potential profile at $P^{\pm}$ states.

[45–49]. In a previous report, we could demonstrate the FE property of MgZnO tunneling barriers [33], by investigating the tunneling electroresistance TER effect [50–52]. The TER effect could be explained by the shift of CoPt surface potential and the change of barrier height. A second-order phase transition was also found at the FE Curie temperature 316 K, which is close to the bulk value of 350 K.

The schematic of the device and the effect of P on MAE are shown in Fig. 1, together with the electric-field cooling (EFC) procedure employed for this report. Due to the large electric coercivity of MgZnO, the cooling under an electric field from above the MgZnO Curie temperature was used to align P in either direction [Fig. 1(a)] [33]. The reversal of P results in a difference of the equilibrium surface charge at the surfaces of the FM electrodes [Fig. 1(b)]. The charge difference is negative (positive) at the CoPt surface after +EFC (−EFC), due to the formation of a positive (negative) P state [Figs. 1(b) and 1(c)]. Based on the following theoretical and experimental analyses, the interfacial MAE component of CoPt electrode will be perpendicular (in-plane) for a P^+ (P^-) state. Such a large nonvolatile change of MAE is driven by the P modulation of the SOC and the $3d$-$5d$ hybridization.

II. FIRST-PRINCIPLES CALCULATIONS

We modeled the effect of ZnO electric polarization on the interfacial MAE of CoPt by first-principles density functional theory calculations [53]. We used scalar and fully relativistic ultrasoft pseudopotentials (USPPs) [54,55] and a plane-wave basis with the generalized gradient approximation [56]. A

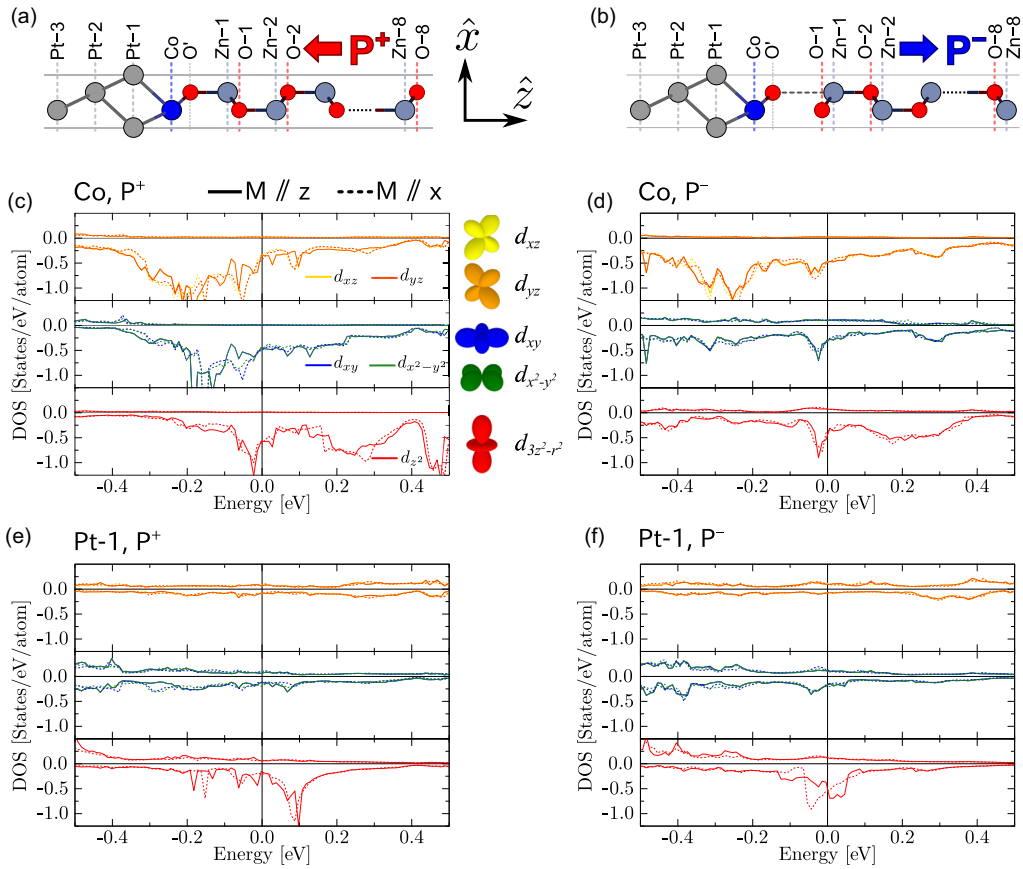

FIG. 2. (a),(b) The model of CoPt/ZnO used for the first-principles calculations, in the (a) P^+ and (b) P^- states. (c)–(f) The projected density of states (PDOS) the (c),(d) Co and (e),(f) Pt-1 atoms in the (c),(e) P^+ and (d),(f) P^- states.

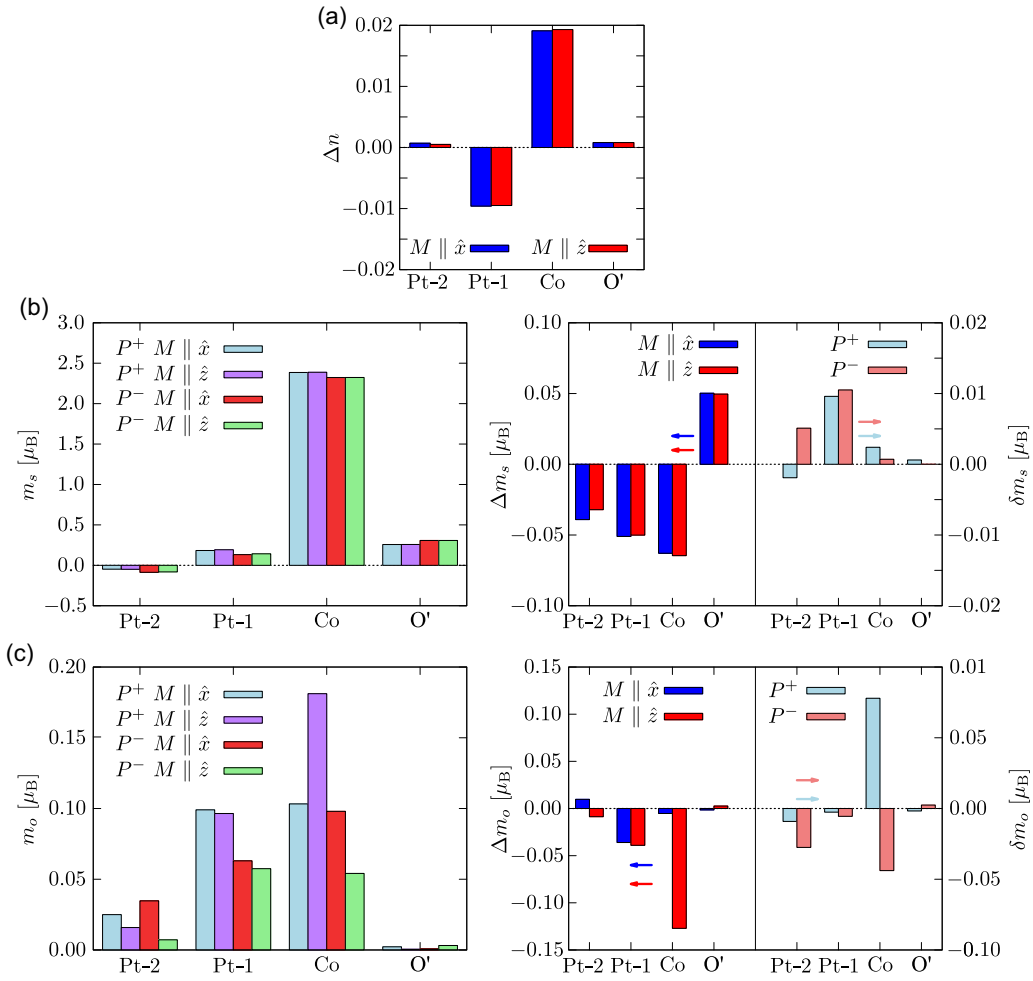

FIG. 3. The layer-resolved values of (a) the change of number of electrons (Δn), (b) the spin momentum (m_s), its change by P (Δm_s), and anisotropy (δm_s), (c) the orbital momentum (m_o), its change by P (Δm_o), and anisotropy (δm_o).

change from a $24 \times 24 \times 1$ mesh to a $32 \times 32 \times 1$ mesh in the k-point sampling space did not show a significant difference in results, and the $32 \times 32 \times 1$ mesh was used. The energy cutoff was set at 30 (300) Ry for the plane-wave basis in wave function (electron density). The structure was vacuum/Pt(3)/Co(1)/O(1)/Zn-O(8)/vacuum (atomic monolayers or bilayers) as shown in Figs. 2(a) and 2(b). The P^+ and P^- states were modeled as either Zn-O or O-Zn bilayers, respectively. The considerations behind the choices for the modeled structure and more details of the calculation methods are available in Ref. [33]. We need to note that the Mg doping and Co-Pt disorder are not taken into account for simplicity, but the main experimental findings could be understood with such a treatment.

The density of states (DOS) was calculated for magnetization orientations at the in-plane $\hat{x}$ and out-of-plane $\hat{z}$ directions for each of P^+ and P^- states [Figs. 2(c)–2(f)]. The calculations incorporate a general SOC with a set of natural multiorbitals, not a simplified SOC limited to the Rashba-type under a minimal orbital set [57,58]. In the following, we define the changes of relevant quantities with respect to P^+ state [$\Delta w = w(P^-) - w(P^+)$], whereas the anisotropy is defined with respect to in-plane direction [$\delta w = w(M\|z) - w(M\|x)$]. At each P state, the MAE was calculated as the difference between the total energies at the in-plane and out-of-plane magnetization M configurations, i.e., $\mathrm{MAE} = E_x - E_z$. The positive and negative signs denote an out-of-plane and in-plane MAE, respectively.

Figures 2(c)–2(f) show a drastic change of DOS. The change of number of electrons (Δn) at the interface Co atom is $+0.02$ [Fig. 3(a)], where the P^+ (P^-) state corresponds to an electron depletion from (doping to) Pt-Co-O interface atoms, as depicted in Fig. 1(b). Surface MAE was $+0.25$ and -1.23 meV/atom for P^+ and P^- states, respectively. These correspond to $+0.44$ and -2.16 erg/cm^2 ($\equiv$ mJ/m^2). The electrons depletion increased the out-of-plane MAE, same as the interfaces of Fe/MgO [11,59–64] and (Fe,Co)/Pt/MgO [65–67]. Although Δn is close in value to an Fe/MgO interface under an electric field of 0.5–1.0 V/nm, the present ΔMAE of -2.60 erg/cm^2 in CoPt/ZnO is much larger than Fe/MgO, which ranges from -0.1 to -0.2 erg/cm^2 [59–61]. Among the 3d-noble metal alloys, calculations showed that CoPt-based systems have the largest electric-field effect on MAE [65,66], but the presented CoPt/ZnO system is showing an even larger effect. Moreover, we need to emphasize that Δn in the present case comes from the electric polarization of ZnO, without the need of a continuously applied voltage as in Fe/MgO.

This large $\Delta MAE/\Delta n$ can be explained by the control of $3d$-$5d$ orbital hybridization of Co/Pt. There is a hybridized peak in $d_{3z^2-r^2}(m=0)$ minority spin DOS that moves near the Fermi level (E_F) with the change of P direction [Figs. 2(e) and 2(f)]. Simultaneously, due to the electric field change, the part of electrons occupying the $3d$ orbitals extending to xy-plane directions ($d_{xz,yz}$ for $|m|=1$ and d_{xy,x^2-y^2} for $|m|=2$) are redistributed into those of $d_{3z^2-r^2}$. This produces a change in orbital and spin momenta of Co and Pt, leading to a large change in DOS and MAE [27,68,69]. Moreover, while the Pt-enhanced SOC of Co is favoring a perpendicular MAE, the P modulation resulted in the closer participation of Pt into the electronic structure at E_F [Fig. 2(f)]. This induces large reductions of orbital momenta on both Co and Pt [Fig. 3(c)], leading to an additional decrease in MAE, due to the strong SOC of Pt. Therefore, even a small Δn in the CoPt/ZnO system gives a strong modulation of MAE.

The DOS sets of $d_{xz,yz}$ and d_{xy,x^2-y^2} orbitals are degenerate in the $M\|\hat{z}$ direction, whereas the degeneracies are lifted when $M\|\hat{x}$ [Figs. 2(c)–2(f)]. At P^+, based on Bruno's model relating to down-down spin scattering [70], both sets and the large SOC contribute strongly to a perpendicular MAE [71]. Correspondingly, the anisotropy in orbital momentum (δm_o) of Co is large at $+0.078\ \mu_B$, supporting the origin of a perpendicular MAE [Fig. 3(c)]. At P^- state, the previously-unoccupied Pt $d_{3z^2-r^2}$ minority peak in DOS is shifted towards E_F, which increases the density of minority spins [Fig. 2(f)]. The application of Bruno's model is limited by the presence of majority states near E_F for both Co and Pt, and an anisotropy in spin momentum ($\delta m_s = +0.010\ \mu_B$) of Pt-1, due to the hybridization change depending on the orientation of M [Fig. 3(b)]. However, δm_o of Co is negative at $-0.044\ \mu_B$, indicating an inplane MAE.

III. MAE OBSERVATIONS FROM RESISTANCE-FIELD CURVES

Experimentally, we estimated MAE in epitaxial stacks of fcc-Pt/fcc-CoPt/w-MgZnO/hcp-Co [32,33]. The (1 1 1)-oriented growth of Pt allows for the growth of MgZnO along the polar c axis, which is suitable to the control of metal surface charge. A relatively-thick bottom electrode was needed for better growth of the MgZnO barrier. Therefore, the deposition conditions and composition of CoPt were chosen to get a value of the magnetocrystalline perpendicular MAE that is close in magnitude to the in-plane shape anisotropy. At such a compensation, the changes in anisotropy at the CoPt/MgZnO interface will be observable, even with a rather thick CoPt layer. The presented experimental results were obtained from samples described previously [32,33]. The initial film structure was made of: c-plane sapphire Al_2O_3 substrate/Pt (30, 700)/$Co_{0.3}Pt_{0.7}$ (10, 500)/$Mg_{0.23}Zn_{0.77}$ (7, 400)/Co (16, 25), where the numbers in parentheses are layer thicknesses in nm and growth temperature in °C, respectively. The Pt and CoPt layers were grown by sputtering deposition, whereas the MgZnO layer was grown from Mg and Zn metallic sources using molecular-beam epitaxy equipped with an oxygen radical source. After that the top Co layer was grown by electron-beam evaporation. The growth of $Co_{0.3}Pt_{0.7}$ at the high temperature of 500 °C is suitable to control the magnetocrystalline perpendicular MAE [24,28–30] and henceforth obtain a very low total MAE.

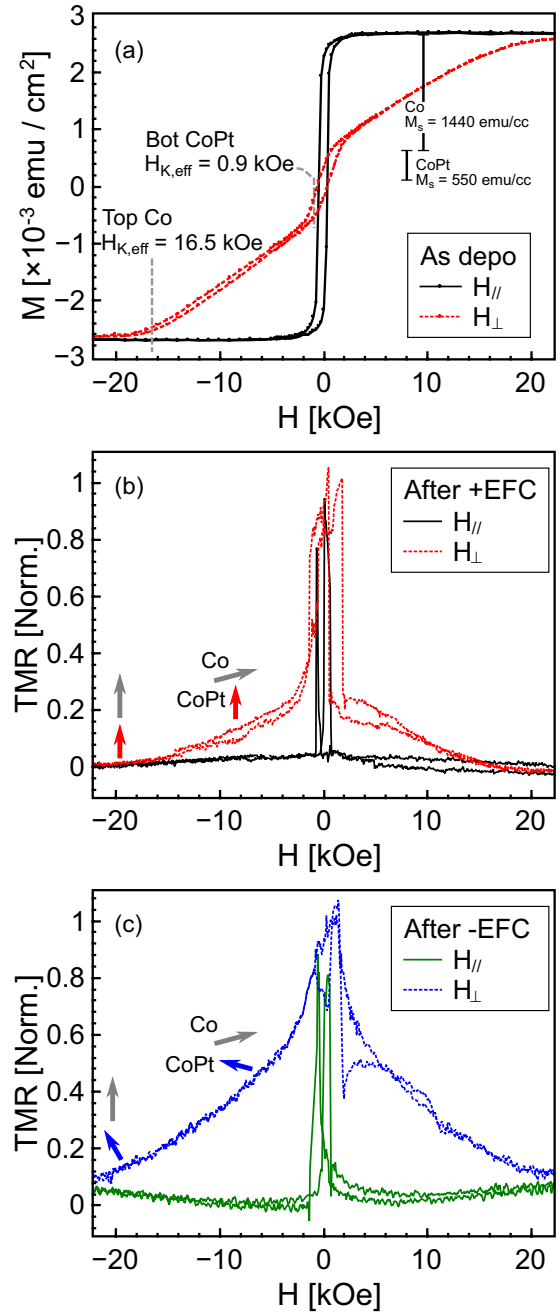

FIG. 4. The experimental effect of P on MAE. (a) The M-H curves in the in-plane $H_\parallel$ and out-of-plane $H_\perp$ directions of the as-deposited state (P^+) of blanket films. The CoPt layer shows a small in-plane total MAE, whereas the Co layer has a dominant in-plane shape MAE. (b),(c) The R-H curves of a fabricated junction in the in-plane and perpendicular directions (b) after $+$EFC at P^+ state, and (c) after $-$EFC at P^- state. The R-H curves indicate that the surface MAE of CoPt changed from the out-of-plane to in-plane direction by P modulation. The measurements in (a) and (b),(c) were done at 5 K and 2 K, respectively.

The unpatterned films were used for magnetic and microstructure characterization. In the as-deposited state,

which corresponds to P^+ state, MAE was estimated from magnetization-field (M-H) curves in unfabricated stacks by a superconducting quantum interference device (SQUID) magnetometer [Fig. 4(a)]. For the fabrication of MTJs and to induce coercivity difference between the top and bottom ferromagnetic layers, the top Co layer was etched down to 2 nm, then $Co_{0.5}Fe_{0.5}$ (2)/IrMn (14)/Ru (5) was deposited *in situ*. After that, the stack was pin annealed for 30 min at 270 °C and a 10-kOe magnetic field. The tunnel junctions were microfabricated by electron-beam lithography and Ar-ion milling. The presented tunneling resistance results are from circular junctions 10 μm in diameter. We measured the tunneling resistance by the four-probe method in a physical-property measurement system. The electrical measurements were at 2 K, after using the EFC procedure to align the MgZnO P (Fig. 1) [33]. The ±EFC from 360 K down to 2 K corresponds to the $P^{\pm}$ states. For MAE observation, the resistance-field (R-H) curves were measured in a field applied consecutively in the $\hat{x}$ and $\hat{z}$ directions.

The M-H curves measured in the in-plane $H_{\parallel}$ and out-of-plane $H_{\perp}$ field directions at 5 K show that the top Co and bottom CoPt layers have an in-plane easy axis at P^+ state [Fig. 4(a)]. However, the bottom CoPt has a small perpendicular saturation field ($H_{\mathrm{K,eff}} = 0.9$ kOe), due to the compensation mentioned above. Figures 4(b) and 4(c) show the normalized R-H curves of the microfabricated MTJs after setting into either of P^+ or P^- states. Due to TER effect, the parallel-state resistance and TMR ratio at zero bias changed from (72 kΩ, +25%) at P^+ state to (380 $k\Omega$, −20%) at P^- state. The normalization was with respect to the same parallel and antiparallel resistances of each P state, to represent the relative angle between CoPt and Co magnetization. The relation between TMR and P will be the scope of another report.

At the P^+ state, the R-H curves show a similar character to the as-deposited M-H curves. In the out-of-plane field direction, there are two shoulders at 1 kOe and 16 kOe, corresponding to $H_{\mathrm{K,eff}}$ of CoPt and Co, respectively. Above the saturation of CoPt at 1 kOe, the CoPt magnetization is out-of-plane, and the Co magnetization rotates towards the out-of-plane direction until saturation at 16 kOe [arrows in Fig. 4(b)]. On the other hand, at P^- state, the corresponding 1-kOe shoulder of CoPt is not present, the slope of R-$H_{\perp}$ at the low-field region decreases, and the area enclosed by in-plane and out-of-plane curves increases [Fig. 4(c)]. This is in accordance with the theory prediction that the CoPt electrode has a large increase of in-plane MAE by P^- state. The surface MAE of CoPt (K_s) can be found from the following relation:

$$K_s = (4\pi M_s - H_{\mathrm{K,eff}}) \times \frac{M_s t}{2}, \tag{1}$$

where M_s is the saturation magnetization, and t is CoPt thickness. We estimate ($H_{\mathrm{K,eff}}$, K_s) = (0.9 kOe, +1.6 erg/cm^2) and (20.0 kOe, −3.6 erg/cm^2) for P^+ and P^- states, respectively. The aforementioned theoretical value of ΔMAE =

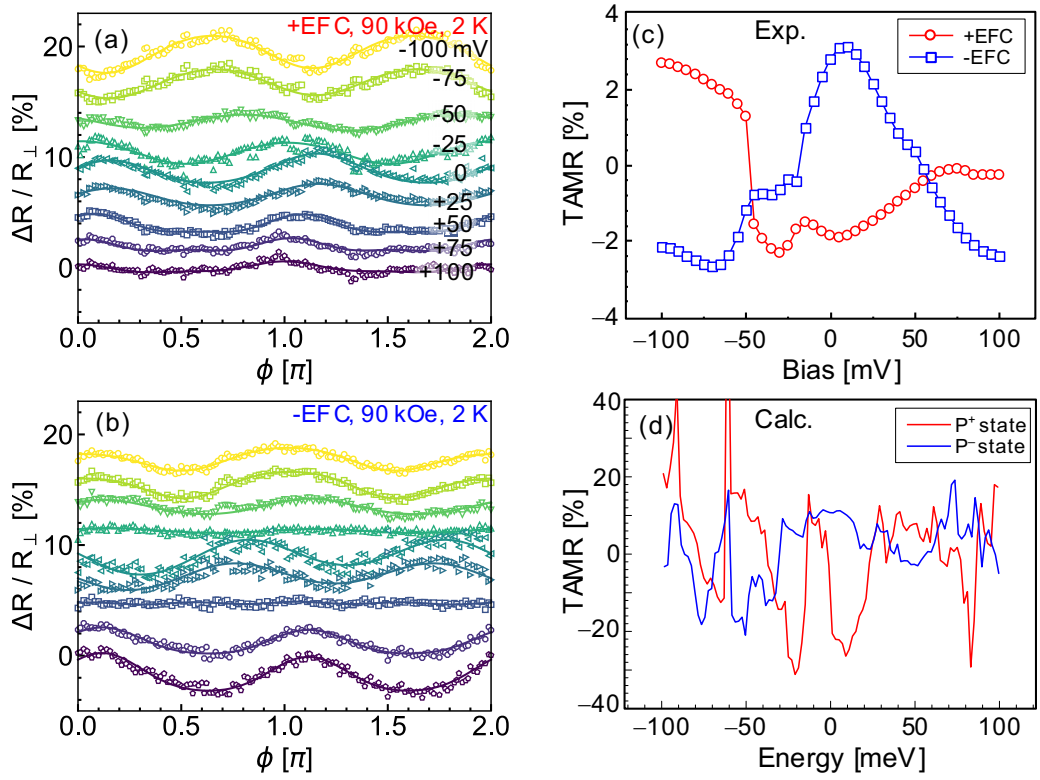

FIG. 5. The effect of P modulation on tunneling anisotropic magnetoresistance (TAMR). (a),(b) Samples of the dependence of TAMR on applied field angle (ϕ) at different bias voltages, (a) after +EFC at P^+ state, and (b) after −EFC at P^- state. The curves are vertically shifted uniformly for clarity. (c) The experimental bias dependence of TAMR. (d) The energy dependence of TAMR from the first-principles calculations. A qualitative agreement is found between the experimental and calculation results.

-2.6 erg/cm^2 has a good agreement with the experimental $\Delta\text{MAE} = -5.2$ erg/cm^2. The direction of change is the same, and the magnitude is within a factor of 2. We need to note that the accuracy of estimating $H_{\text{K,eff}}$ at P^- state can be hindered by an unaccounted for P modulation of the MAE of the top Co electrode. However, the change of R-$H_\perp$ slope and area is an indication of the change of K_s at CoPt electrode. Further experimental confirmations on bilayers of CoPt/MgZnO should be employed, e.g., gated anomalous Hall effect [7], magnetic moment measurement under electric field [8], or x-ray absorption spectroscopy [62].

IV. TUNNELING ANISOTROPIC MAGNETORESISTANCE

The magnetocrystalline anisotropy is determined by the occupied and unoccupied states close to the Fermi level. In a related manner, an anisotropy in DOS (ADOS) by M rotation makes the tunneling current dependent on M direction, the named tunneling anisotropic magnetoresistance (TAMR) [72,73]. As the TAMR and MAE are both related to DOS at the Fermi level, the investigation of TAMR around zero bias can put light on MAE [74] and confirm that the first-principles calculations explain the mechanism of MAE. We expect that due to the electric field at the interface, the TAMR will be affected largely by the P^+ and P^- states.

In the present case, the symmetry-selective filtering of tunneling current is not evident, and TAMR in CoPt-based tunnel junctions can be understood qualitatively in terms of ADOS at the interface next to the tunneling barrier [73,75]. We define ADOS as $\text{DOS}(M\|z)/\text{DOS}(M\|x)-1$. Between the two P states, the calculations showed a change of which orbitals set produces the ADOS character (Fig. 2). The anisotropy is mainly in the minority spin and shows an origin similar to MAE. For P^+ (P^-) state, ADOS is mainly from $d_{xz,yz}$ and d_{xy,x^2-y^2} ($d_{3z^2-r^2}$) orbitals. Because of this, the total ADOS representing TAMR changes the sign at the Fermi level from negative at P^+ state to positive at P^- [Fig. 5(d)].

For the TAMR experimental measurements, the out-of-plane angular dependence of differential resistance (R-ϕ) was measured at various bias voltages and a fixed field of 90 kOe, which is much higher than saturation. The chosen bias range of ± 0.1 V is smaller than the 0.7–1.0 V required to induce P change. The definition of ϕ is such that $\phi = 0$ and $\pi/2$ correspond to $M\|z$ and $M\|x$, respectively. Similar to the calculations definition, TAMR ratio is defined as $R(\phi = \pi/2)/R(0) - 1$. Figures 5(a) and 5(b) show that R is anisotropic in ϕ, and the character of TAMR-ϕ curves at different biases are changed by the P state. Fittings to R-ϕ curves were used to extract the twofold component of TAMR, and the bias dependence is shown in Fig. 5(c). Close to zero bias, the TAMR changes the sign from negative at P^+ state to positive at P^-.

A qualitative agreement between experiments and calculations in TAMR sign is found. For both calculations and experiment, TAMR at the Fermi level is negative (positive) at the P^+ (P^-) state. The origin for TAMR sign change is related to the sign change of Co's δm_o, henceforth ΔMAE [rightmost panel of Fig. 3(c)]. The fine details of TAMR spectra can be modified by Co-Pt disorder, but the mechanism is captured by the simplified first-principles calculations in CoPt/ZnO hexagonal system.

V. CONCLUSIONS

In summary, by first-principles calculations and experimental measurements, we investigated the large control of MAE of CoPt ferromagnet by the electric polarization of the wurtzite MgZnO tunnel barrier. The surface MAE sign changed, with a difference in magnitude that is much larger than Fe/MgO. A combined study of MAE and TAMR showed consistent results from both experiments and calculations. Therefore, we consider that the TAMR observations are important for the explanation of ΔMAE. The origin is likely due to the control of DOS and SOC in the CoPt interface by the modulation of $3d$-$5d$ hybridization driven by ZnO polarization. This shows the possibility of designing large nonvolatile voltage control of MAE.

As a final note on possible applications, the ZnO polarization can be used either as an amplifier for low-voltage control of MAE, or for nonvolatile gating of MAE. One possibility is in the toggle-type voltage magnetic random-access memories (V-MRAM) [12,14]. An alternating $+-+$ voltage pulse can be used for the precessional magnetization switching, similar to what is proposed for non-FE barriers [76]. In the VCMA-assisted spin-orbit-torque writing [77], we propose that a single voltage pulse can be used for nonvolatile bit selection/deactivation in Pt/CoPt/ZnO structures. The other bits do not require manipulation, therefore making the scheme much simpler. Another favorable application is the utilization of nonvolatile control of MAE in reconfigurable spin-wave logic devices [78]. Therefore, we believe that the present work should open a way for applications in nonvolatile energy-efficient control of magnetic memories and information processing.

ACKNOWLEDGMENTS

The authors are thankful to Haruyuki Endo of Iwate Industrial Research Institute, Japan for helping in the samples preparation. This work was partially supported by the JSPS Grant No. JP13J05806, the JSPS KAKENHI Grant No. JP18K04923, Kanazawa University SAKIGAKE Project, the Computational Materials Science Initiative, Japan, the Advanced Institute for Computational Science and Information Technology Center of Nagoya University through the High Performance Computing Infrastructure (HPCI) System Research Project under Projects hp17168 and hp180206, and the ImPACT Program of the Council for Science, Technology and Innovation (Cabinet Office, Government of Japan). The first-principles calculations were performed using the facilities of the Supercomputer Center, Institute for Solid State Physics, University of Tokyo, Japan.

M.A.-M., M.B., and M.O. contributed equally to this work.

[1] F. Matsukura, Y. Tokura, and H. Ohno, Nat. Nanotechnol. **10**, 209 (2015).

[2] C. Song, B. Cui, F. Li, X. Zhou, and F. Pan, Prog. Mater. Sci. **87**, 33 (2017).

[3] H. Ohno, D. Chiba, F. Matsukura, T. Omiya, E. Abe, T. Dietl, Y. Ohno, and K. Ohtani, Nature (London) **408**, 944 (2000).

[4] D. Chiba, S. Fukami, K. Shimamura, N. Ishiwata, K. Kobayashi, and T. Ono, Nat. Mater. **10**, 853 (2011).

[5] D. Chiba, M. Yamanouchi, F. Matsukura, and H. Ohno, Science **301**, 943 (2003).

[6] M. Weisheit, S. Fähler, A. Marty, Y. Souche, C. Poinsignon, and D. Givord, Science **315**, 349 (2007).

[7] M. Endo, S. Kanai, S. Ikeda, F. Matsukura, and H. Ohno, Appl. Phys. Lett. **96**, 212503 (2010).

[8] A. Obinata, Y. Hibino, D. Hayakawa, T. Koyama, K. Miwa, S. Ono, and D. Chiba, Sci. Rep. **5**, 14303 (2015).

[9] V. Garcia, M. Bibes, L. Bocher, S. Valencia, F. Kronast, A. Crassous, X. Moya, S. Enouz-Vedrenne, A. Gloter, D. Imhoff, C. Deranlot, N. D. Mathur, S. Fusil, K. Bouzehouane, and A. Barthélémy, Science **327**, 1106 (2010).

[10] D. Chiba, M. Sawicki, Y. Nishitani, Y. Nakatani, F. Matsukura, and H. Ohno, Nature (London) **455**, 515 (2008).

[11] T. Maruyama, Y. Shiota, T. Nozaki, K. Ohta, N. Toda, M. Mizuguchi, A. A. Tulapurkar, T. Shinjo, M. Shiraishi, S. Mizukami, Y. Ando, and Y. Suzuki, Nat. Nanotechnol. **4**, 158 (2009).

[12] Y. Shiota, T. Nozaki, F. Bonell, S. Murakami, T. Shinjo, and Y. Suzuki, Nat. Mater. **11**, 39 (2011).

[13] W.-G. Wang, M. Li, S. Hageman, and C. L. Chien, Nat. Mater. **11**, 64 (2012).

[14] S. Kanai, M. Yamanouchi, S. Ikeda, Y. Nakatani, F. Matsukura, and H. Ohno, Appl. Phys. Lett. **101**, 122403 (2012).

[15] H. X. Yang, M. Chshiev, B. Dieny, J. H. Lee, A. Manchon, and K. H. Shin, Phys. Rev. B **84**, 054401 (2011).

[16] P. K. Amiri, J. G. Alzate, X. Q. Cai, F. Ebrahimi, Q. Hu, K. Wong, C. Grèzes, H. Lee, G. Yu, X. Li, M. Akyol, Q. Shao, J. A. Katine, J. Langer, B. Ocker, and K. L. Wang, IEEE Trans. Magn. **51**, 1 (2015).

[17] C. Grezes, H. Lee, A. Lee, S. Wang, F. Ebrahimi, X. Li, K. Wong, J. A. Katine, B. Ocker, J. Langer, P. Gupta, P. K. Amiri, and K. L. Wang, IEEE Magn. Lett. **8**, 1 (2017).

[18] Y. Shiota, T. Nozaki, S. Tamaru, K. Yakushiji, H. Kubota, A. Fukushima, S. Yuasa, and Y. Suzuki, Appl. Phys. Lett. **111**, 022408 (2017).

[19] C.-G. Duan, J. P. Velev, R. F. Sabirianov, W. N. Mei, S. S. Jaswal, and E. Y. Tsymbal, Appl. Phys. Lett. **92**, 122905 (2008).

[20] A. Mardana, S. Ducharme, and S. Adenwalla, Nano Lett. **11**, 3862 (2011).

[21] P. V. Lukashev, J. D. Burton, S. S. Jaswal, and E. Y. Tsymbal, J. Phys.: Condens. Matter **24**, 226003 (2012).

[22] P. V. Lukashev, T. R. Paudel, J. M. López-Encarnación, S. Adenwalla, E. Y. Tsymbal, and J. P. Velev, ACS Nano **6**, 9745 (2012).

[23] M. Lee, H. Choi, and Y.-C. Chung, J. Appl. Phys. **113**, 17C729 (2013).

[24] W. Grange, M. Maret, J.-P. Kappler, J. Vogel, A. Fontaine, F. Petroff, G. Krill, A. Rogalev, J. Goulon, M. Finazzi, and N. B. Brookes, Phys. Rev. B **58**, 6298 (1998).

[25] O. N. Mryasov, U. Nowak, K. Y. Guslienko, and R. W. Chantrell, EPL (Europhysics Letters) **69**, 805 (2005).

[26] A. B. Shick, F. Máca, M. Ondráček, O. N. Mryasov, and T. Jungwirth, Phys. Rev. B **78**, 054413 (2008).

[27] A. Sakuma, J. Phys. Soc. Jpn. **63**, 3053 (1994).

[28] D. Weller, H. Brändle, G. Gorman, C.-J. Lin, and H. Notarys, Appl. Phys. Lett. **61**, 2726 (1992).

[29] P. W. Rooney, A. L. Shapiro, M. Q. Tran, and F. Hellman, Phys. Rev. Lett. **75**, 1843 (1995).

[30] M. Maret, M. Cadeville, R. Poinsot, A. Herr, E. Beaurepaire, and C. Monier, J. Magn. Magn. Mater. **166**, 45 (1997).

[31] M. Belmoubarik, T. Nozaki, H. Endo, and M. Sahashi, J. Appl. Phys. **113**, 17C106 (2013).

[32] M. Belmoubarik, M. Al-Mahdawi, H. Sato, T. Nozaki, and M. Sahashi, Appl. Phys. Lett. **106**, 252403 (2015).

[33] M. Belmoubarik, M. Al-Mahdawi, M. Obata, D. Yoshikawa, H. Sato, T. Nozaki, T. Oda, and M. Sahashi, Appl. Phys. Lett. **109**, 173507 (2016).

[34] A. B. Shick and O. N. Mryasov, Phys. Rev. B **67**, 172407 (2003).

[35] A. K. Tagantsev, Appl. Phys. Lett. **93**, 202905 (2008).

[36] J. W. Bennett, K. F. Garrity, K. M. Rabe, and D. Vanderbilt, Phys. Rev. Lett. **109**, 167602 (2012).

[37] H. Moriwake, A. Konishi, T. Ogawa, K. Fujimura, C. A. J. Fisher, A. Kuwabara, T. Shimizu, S. Yasui, and M. Itoh, Appl. Phys. Lett. **104**, 242909 (2014).

[38] T. S. Herng, A. Kumar, C. S. Ong, Y. P. Feng, Y. H. Lu, K. Y. Zeng, and J. Ding, Sci. Rep. **2**, 587 (2012).

[39] Y. C. Yang, C. Song, F. Zeng, F. Pan, Y. N. Xie, and T. Liu, Appl. Phys. Lett. **90**, 242903 (2007).

[40] Y. C. Yang, C. Song, X. H. Wang, F. Zeng, and F. Pan, J. Appl. Phys. **103**, 074107 (2008).

[41] A. Onodera and M. Takesada, in *Advances in Ferroelectrics*, edited by A. Peliz-Barranco (InTech, London, 2012).

[42] R. Joshi, P. Kumar, A. Gaur, and K. Asokan, Appl. Nanosci. **4**, 531 (2013).

[43] J. Lee, N. Subramaniam, T. Kang, Y. Shon, and E. Kim, Solid State Commun. **209-210**, 11 (2015).

[44] J. Xiao, T. S. Herng, J. Ding, and K. Zeng, Acta Mater. **123**, 394 (2017).

[45] A. Onodera, N. Tamaki, K. Jin, and H. Yamashita, Jpn. J. Appl. Phys. **36**, 6008 (1997).

[46] J. G. Lu, S. Fujita, T. Kawaharamura, H. Nishinaka, Y. Kamada, and T. Ohshima, Appl. Phys. Lett. **89**, 262107 (2006).

[47] Dhananjay and S. B. Krupanidhi, Appl. Phys. Lett. **89**, 082905 (2006).

[48] Y. Kozuka, A. Tsukazaki, and M. Kawasaki, Appl. Phys. Rev. **1**, 011303 (2014).

[49] P. Kumar, J. P. Singh, H. K. Malik, S. Gautam, K. Chae, and K. Asokan, Superlattices Microstruct. **78**, 183 (2015).

[50] M. Y. Zhuravlev, R. F. Sabirianov, S. S. Jaswal, and E. Y. Tsymbal, Phys. Rev. Lett. **94**, 246802 (2005).

[51] A. Gruverman, D. Wu, H. Lu, Y. Wang, H. W. Jang, C. M. Folkman, M. Y. Zhuravlev, D. Felker, M. Rzchowski, C.-B. Eom, and E. Y. Tsymbal, Nano Lett. **9**, 3539 (2009).

[52] V. Garcia and M. Bibes, Nat. Commun. **5**, 4289 (2014).

[53] P. Hohenberg and W. Kohn, Phys. Rev. **136**, B864 (1964).

[54] D. Vanderbilt, Phys. Rev. B **41**, 7892 (1990).

[55] M. Tsujikawa, A. Hosokawa, and T. Oda, Phys. Rev. B **77**, 054413 (2008).

[56] J. P. Perdew, J. A. Chevary, S. H. Vosko, K. A. Jackson, M. R. Pederson, D. J. Singh, and C. Fiolhais, Phys. Rev. B **46**, 6671 (1992).

[57] S. E. Barnes, J. Ieda, and S. Maekawa, Sci. Rep. **4**, 4105 (2014).
[58] K.-W. Kim, K.-J. Lee, H.-W. Lee, and M. D. Stiles, Phys. Rev. B **94**, 184402 (2016).
[59] K. Nakamura, T. Akiyama, T. Ito, M. Weinert, and A. J. Freeman, Phys. Rev. B **81**, 220409(R) (2010).
[60] M. K. Niranjan, C.-G. Duan, S. S. Jaswal, and E. Y. Tsymbal, Appl. Phys. Lett. **96**, 222504 (2010).
[61] D. Yoshikawa, M. Obata, Y. Taguchi, S. Haraguchi, and T. Oda, Appl. Phys. Exp. **7**, 113005 (2014).
[62] S. Miwa, K. Matsuda, K. Tanaka, Y. Kotani, M. Goto, T. Nakamura, and Y. Suzuki, Appl. Phys. Lett. **107**, 162402 (2015).
[63] T. Nozaki, A. Kozioł-Rachwał, W. Skowroński, V. Zayets, Y. Shiota, S. Tamaru, H. Kubota, A. Fukushima, S. Yuasa, and Y. Suzuki, Phys. Rev. Applied **5**, 044006 (2016).
[64] Q. Xiang, Z. Wen, H. Sukegawa, S. Kasai, T. Seki, T. Kubota, K. Takanashi, and S. Mitani, J. Phys. D: Appl. Phys. **50**, 40LT04 (2017).
[65] H. Zhang, M. Richter, K. Koepernik, I. Opahle, F. Tasnádi, and H. Eschrig, New J. Phys. **11**, 043007 (2009).
[66] M. Tsujikawa, S. Haraguchi, and T. Oda, J. Appl. Phys. **111**, 083910 (2012).
[67] S. Miwa, M. Suzuki, M. Tsujikawa, K. Matsuda, T. Nozaki, K. Tanaka, T. Tsukahara, K. Nawaoka, M. Goto, Y. Kotani, T. Ohkubo, F. Bonell, E. Tamura, K. Hono, T. Nakamura, M. Shirai, S. Yuasa, and Y. Suzuki, Nat. Commun. **8**, 15848 (2017).
[68] G. H. O. Daalderop, P. J. Kelly, and M. F. H. Schuurmans, Phys. Rev. B **42**, 7270 (1990).
[69] G. H. O. Daalderop, P. J. Kelly, and M. F. H. Schuurmans, Phys. Rev. B **50**, 9989 (1994).
[70] P. Bruno, Phys. Rev. B **39**, 865 (1989).
[71] D.-s. Wang, R. Wu, and A. J. Freeman, Phys. Rev. B **47**, 14932 (1993).
[72] C. Gould, C. Rüster, T. Jungwirth, E. Girgis, G. M. Schott, R. Giraud, K. Brunner, G. Schmidt, and L. W. Molenkamp, Phys. Rev. Lett. **93**, 117203 (2004).
[73] B. G. Park, J. Wunderlich, D. A. Williams, S. J. Joo, K. Y. Jung, K. H. Shin, K. Olejník, A. B. Shick, and T. Jungwirth, Phys. Rev. Lett. **100**, 087204 (2008).
[74] H. Saito, S. Yuasa, and K. Ando, Phys. Rev. Lett. **95**, 086604 (2005).
[75] A. B. Shick, F. Máca, J. Mašek, and T. Jungwirth, Phys. Rev. B **73**, 024418 (2006).
[76] T. Ikeura, T. Nozaki, Y. Shiota, T. Yamamoto, H. Imamura, H. Kubota, A. Fukushima, Y. Suzuki, and S. Yuasa, Jpn. J. Appl. Phys. **57**, 040311 (2018).
[77] H. Yoda, N. Shimomura, Y. Ohsawa, S. Shirotori, Y. Kato, T. Inokuchi, Y. Kamiguchi, B. Altansargai, Y. Saito, K. Koi, H. Sugiyama, S. Oikawa, M. Shimizu, M. Ishikawa, K. Ikegami, and A. Kurobe, in *2016 IEEE International Electron Devices Meeting (IEDM)* (IEEE, USA, 2016), pp. 27.6.1–27.6.4.
[78] B. Rana and Y. C. Otani, Phys. Rev. Applied **9**, 014033 (2018).